

1

2 ***Brief Communication:***

3 **Contending estimates of 2003-2008 glacier mass balance**
4 **over the Pamir-Karakoram-Himalaya**

5
6 Andreas Kääb¹, Désirée Treichler¹, Christopher Nuth¹, Etienne Berthier²

7
8 [1] {Department of Geosciences, University of Oslo, P.O. Box 1047, Oslo, Norway}

9 [2] {CNRS, Université de Toulouse, LEGOS, 14 avenue Ed. Belin, Toulouse 31400, France }

10 Correspondence to: Andreas Kääb (kaeab@geo.uio.no)

11
12 **Abstract**

13 We present glacier thickness changes over the entire Pamir-Karakoram-Himalaya arc based
14 on ICESat satellite altimetry data for 2003-2008. We highlight the importance of C-band
15 penetration for studies based on the SRTM elevation model. This penetration seems to be of
16 potentially larger magnitude and variability than previously assumed. The most negative rate
17 of region-wide glacier elevation change ($< -1 \text{ m yr}^{-1}$) is observed for the East
18 Nyainqêntanglha Shan. Conversely, glaciers of the West Kunlun Shan are slightly gaining
19 volume, and Pamir and Karakoram seem to be on the western edge of this mass gain anomaly
20 rather than its centre. For the Ganges, Indus and Brahmaputra basins, the glacier mass change
21 reaches $-22 \pm 3 \text{ Gt yr}^{-1}$, about 10% of the current glacier contribution to sea-level rise. For
22 selected catchments, we estimate glacier imbalance contributions to river runoff from a few
23 percent to greater than 10%.

25

1 Introduction and Methods

26

27

28

29

30

31

32

33

34

Region-wide measurements of glacier volume or mass change are limited for the Pamir-Karakoram-Himalaya region, leaving room for speculation about the glacier response to climate change and its hydrological significance. Glacier mass change in high mountain Asia (or some part of it) have been obtained by (i) extrapolating the few existing in-situ mass balance series (Cogley, 2011; Bolch et al., 2012; Yao et al., 2012), (ii) using space gravimetry (Jacob et al., 2012; Gardner et al., 2013), (iii) laser altimetry (Kääb et al., 2012; Gardner et al., 2013; Neckel et al., 2014), and (iv) the differencing of digital elevation models (Gardelle et al., 2013). Between these studies that narrow down the range of uncertainties for core parts of this remote mountain region, significant inconsistencies remain.

35

36

37

38

39

The aims of this study are to provide (i) a new consistent regional-scale data set from the ICESat autumn laser campaigns (2003-2008) by extending Kääb et al. (2012) to completely cover the study region by Gardelle et al. (2013) and several major river basins, (ii) to compare the results to other previous estimates of the Pamir-Karakoram-Himalaya glacier volume change, and (iii) to roughly evaluate the contribution of glacier mass change to river runoff.

40

41

42

43

44

45

46

47

48

49

50

51

52

We follow the methods explained in Kääb et al. (2012) with a considerable extension towards the East Nyainqêntanglha Shan, the Pamir and part of the Tibetan Plateau (Fig. 1). In short, ICESat footprints are intersected with the February 2000 SRTM DEM and overlaid on the most snow-free multispectral Landsat images over ~2000-2013 to manually classify footprints into three classes; glaciers, non-glaciers and water. Glacier elevation difference trends are then estimated regionally and at a $1^\circ \times 1^\circ$ geographic grid by fitting a robust linear temporal trend to the time series of elevation differences between the SRTM DEM and individual ICESat footprint elevations. Trends are derived from autumn ICESat campaigns only (2009 ICESat winter campaigns excluded), because combined autumn and winter trends are sensitive to temporal variations in accumulation amount and timing, potentially introducing bias (see Supplement of Kääb et al., 2012). We confirm that our trends are not due to sampling bias of ICESat elevations by comparing ICESat elevation histograms with glacier hypsometry. The resulting elevation difference trends for all our zones are given in Tab. 1.

2 Glacier thickness changes

2.1 Thickening in the Karakoram and West Kunlun Shan

A first striking feature in the regional map of elevation difference trends (Fig. 1) is glacier thickness gain in the West Kunlun Shan ($\sim +0.1 \text{ m yr}^{-1}$), agreeing with in-situ mass balance and length change measurements (Yao et al., 2012). There is a southwest to northeast gradient from considerably negative glacier mass balances in Hindu Kush and Spiti Lahaul to positive values in the Pamir-Karakoram-West Kunlun Shan region (Fig. 1). This suggests the so-called Karakoram glacier mass-balance anomaly (Hewitt, 2011; Gardelle et al., 2012), or Pamir-Karakoram anomaly (Gardelle et al., 2013), is rather the edge or southwest limit of an anomaly centred more to the northeast over the West Kunlun Shan, or Tarim Basin. The anomaly seems thus indeed the result of a larger-scale meteorological or climatic feature, and peculiarities of the Karakoram topography or glaciers (e.g., surge type, hypsometry, avalanche contribution; Hewitt, 2011) do not necessarily play a decisive role. Combined, the results by Gardner et al. (2013), Neckel et al. (2014), and the glacier elevation change pattern of Fig. 1 suggest the centre of the anomaly could be located over the Tibetan Plateau.

Direct precipitation measurements in this region are scarce thus trends are uncertain. Satellite-retrieved precipitation and gauge data (Global Precipitation Climatology Project) suggest an increase of precipitation over the study region north of Karakoram and east of Pamir (Yao et al., 2012). Chinese measurements show increased precipitation over the Tibetan Plateau (personal communication Chong-Yu Xu), and Tao et al. (2014) suggest wetter conditions over the Tarim Basin since the mid 1980s. A number of abnormally wet years occurred during the early 21st century over the Tarim Basin and the Tibetan Plateau (Becker et al., 2013), in particular for the hydrological years 2003/4 and 2005/6. A recent climate modelling study proposes that stable or increasing snowfalls characterise the Karakoram anomaly on a background of increasing air temperatures (Kapnick et al., 2014). Despite the available studies and data, further research seems necessary to consolidate the precipitation and temperature trends, and the reason behind the slight glacier volume gains.

2.2 Massive thinning in East Nyainqêntanglha Shan and Spiti Lahaul

The other striking feature in Fig. 1 is the massive glacier thickness loss in the East Nyainqêntanglha Shan (between -1 m yr^{-1} and -1.7 m yr^{-1}), also consistent with the large negative mass balances and frontal retreats in this zone (Yao et al., 2012). The glaciers of East Nyainqêntanglha Shan have the smallest total elevational range in our study region, indicating

85 a large sensitivity to fluctuations in the equilibrium line altitude (Pelto, 2010; Loibl et al.,
86 2014). The few available in-situ mass balance measurements in the area suggest that the
87 equilibrium line was over the vertical limits of the monitored glaciers in the late 2000s, and
88 precipitation in this zone shows the strongest long-term decrease over the entire Pamir-
89 Karakoram-Himalaya region (Yao et al., 2012; Becker et al. 2013). A similar pattern of
90 glacier shrinkage, though less distinct, is found at the western end of the Great Himalaya
91 Range within our Spiti Lahaul zone and forms the cluster of second-largest thickness loss
92 rates in this study (-0.5 to -0.7 m yr⁻¹). Also here, Landsat data indicate that firn lines have in
93 several years risen towards high glacier elevations resulting in very small accumulation areas
94 or even their complete loss.

95 The 2003-2008 glacier thickness changes in the other study zones are all similar, on the order
96 of ~ -0.4 to -0.5 m yr⁻¹ (Tab.1), with more negative values in the Bhutan zone at the transition
97 between the East Nyaiqêntanglha and Everest zones. We note that glaciers dominated by the
98 summer monsoon (i.e. east of the Spiti Lahaul) all show thickness losses (summer-
99 accumulation type glaciers; Fujita, 2008; Kapnick et al., 2014; Maussion et al., 2014). East
100 Nyaiqêntanglha Shan, the zone with strongest glacier thickness loss, receives most
101 accumulation during March-May (spring-accumulation type; Maussion et al., 2014). The
102 glaciers with considerable winter accumulation under influence of the Westerlies show a more
103 mixed picture with stable or growing thicknesses in the Karakoram and West Kunlun Shan,
104 but thickness losses for instance in the Hindu Kush.

105 **2.3 Comparison to previous thickness change studies**

106 The following comparison to other studies uses average glacier thickness changes rather than
107 total mass changes in order to minimize effects from different delineations of study zones,
108 glacier cover areas, and density assumptions. From Hindu Kush and Karakoram in the west to
109 Nepal in the east, results of all studies agree within their errors (Tab.1). Results are most
110 sensitive to zone delineation in the Hindu Kush, reflecting the strong spatial variability of
111 glacier thickness change rates in this area (Fig. 1) and presumably also locally heterogeneous
112 glacier behaviour (Sarıkaya et al., 2012; see also below for Pamir).

113 Significant differences between the results of all studies are found over East Nyainqêntanglha
114 Shan. Our results and those from Neckel et al. (2014) agree within the errors, but not with
115 Gardner et al. (2013) although all three studies are based on ICESat. While our study and
116 Neckel et al. use ICESat footprint classifications from contemporary satellite images, Gardner
117 et al. use Randolph Glacier Inventory outlines (RGI version 2.0; Pfeffer et al., 2014), which

118 contain considerable errors of commission and omission in this zone (see Table 1 in Gardelle
119 et al., 2013). Repeating our analysis with footprint classifications based on the Randolph
120 Glacier Inventory results in less negative elevation difference trends on glaciers (~ 20% less
121 negative) due to inclusion of non-glacier footprints. Vice versa, the elevation difference trends
122 on land are close to 0 when using our own footprint classification, but become negative if
123 ICESat footprints are classified using RGI due to inclusion of glacier footprints. The
124 remaining discrepancy is presumably due to the fact that the ICESat-based results of Gardner
125 et al. (2013) are averaged from three different methods. Their results based on autumn
126 footprints only (method B, Gardner et. al., 2013) suggest a thickness change rate of -0.86 m yr^{-1} ,
127 which is in closer agreement with our results.

128 At a first glance, East Nyainqêntanglha Shan results from Gardelle et al. (2013; zone called
129 there Hengduan Shan) and Gardner et al. (2013) seem to agree, but we believe this might be a
130 coincidence. First, above we argue why the Gardner et al. (2013) results might be less
131 negative. Second, the results in Gardelle et al. (2013) rely crucially on an estimate of SRTM
132 C-band penetration. Over any glacier globally, the SRTM radar waves will typically have
133 penetrated into the snow and ice, with potential largest penetration depths through snow and
134 firn, and smallest through ice (Kääb et al, 2012; Dall et al., 2001; Rignot et al. 2001). As a
135 consequence, SRTM glacier elevations do not, in general, reflect real mid-February 2000
136 glacier surface elevations but some lower horizon, the elevation of which depends among
137 others on the dielectric properties and structure of the penetrated glacier volume during the
138 SRTM campaign. For elevation difference studies where one of the elevation data sets is the
139 SRTM, its penetration depth needs to be estimated for correction, and biases in this estimate
140 translate directly into offsets in thickness change. Gardelle et al. (2013) used an average C-
141 band penetration of 1.7 m for East Nyainqêntanglha Shan estimated from the difference of
142 SRTM C-band and X-band DEMs (Gardelle et al., 2012). Here, we extrapolate our ICESat
143 elevation trends over 2003-2008 and their uncertainty back in time to the SRTM acquisition
144 period in February 2000. Under the coarse assumption that the 2000-2003 trends equal the
145 2003-2008 ones, the extrapolation should at February 2000 result in a zero elevation
146 difference to ICESat since the SRTM DEM was used as elevation reference. Offsets in this
147 elevation difference for February 2000 are mainly attributed to SRTM radar penetration into
148 ice and snow (for method and discussion see Kääb et al., 2012). For East Nyainqêntanglha
149 Shan this analysis indicates an average penetration of 8-10 m (7-9 m if based on the winter
150 trends that might alternatively be assumed to reflect February conditions), much more than
151 the 1.7 m assumed in Gardelle et al. (2013), while the corresponding off-glacier penetration is

152 not discernible from zero. Clearly, our penetration depth lies at the high end, but remains
153 within the range of possible C-band phase-centre penetrations (Kääb et al, 2012, Dall et al.,
154 2001, Rignot et al. 2001). Sakai et al. (2014) suggest the highest accumulation rates of the
155 entire study region occur in East Nyainqêntanglha Shan, together with Hindu Kush.
156 Correction of the Gardelle et al. (2013) results by our present C-band penetration estimate
157 completely reconciles their results with ours. Note, however, that extrapolation of our 2003-
158 2008 elevation difference trend back to 2000 is based on the risky assumption that the 2000-
159 2003 trend equals the 2003-2008 trend.

160 For the Bhutan zone, Gardelle et al. (2013) estimated a C-band penetration for February 2000
161 of 2.4 m whereas our extrapolation of ICESat trends suggests around 6 m, which again
162 reconciles the results of both studies for this zone.

163 In the Pamir, our results are more negative than Gardner et al. (2013) and in particular
164 Gardelle et al. (2013). As above, we suggest that our manual classification of ICESat
165 footprints versus the Randolph Glacier Inventory contributed to the difference between this
166 study and Gardner et al. (2013; remark: Gardelle et al., 2013, used their own inventory). Also,
167 the difference between our study and Gardner et al. (2013) is reduced if only the results from
168 their Method B (similar to ours) is considered. Gardelle et al. (2013) find glacier thickness
169 changes of $+0.16 \pm 0.15$ m yr⁻¹ over the Pamir whereas the present study suggests $-0.48 \pm$
170 0.08 m yr⁻¹. Again, we find larger SRTM C-band penetration of 5-6 m compared to 1.8 m
171 (Gardelle et al., 2013). Applying the average C-band penetration from the present study again
172 reconciles the results of both studies. However, comparison of both studies in Pamir is
173 complicated by a number of glacier surges (Gardelle et al., 2013) in connection with
174 particularly sparse ICESat glacier coverage. Superimposing ICESat tracks over Landsat
175 images and the elevation change map of Gardelle et al. (2013) reveals that they cross areas of
176 either strongly positive or negative elevation change zones from surge waves. The ICESat
177 trends thus become biased depending on where they sample surges, and the total ICESat
178 sample size over Pamir is not large enough to compensate for these effects. The different
179 observation periods for both studies (2000-2011 versus 2003-2008) may also have
180 considerable impact due to surge activities and climate inter-annual variability (Yi and Sun,
181 2014).

3 Glacier mass changes and water resources

We assume an average density of 850 kg m^{-3} for all 2003-2008 volume changes to convert the thickness changes to water equivalent quantities (Huss, 2013; see Kääb et al., 2012, for different density scenarios). The total glacier area is estimated using a simple cross-product: we multiply the number of ICESat glacier footprints in each zone with the ratio between the total zone area and total number of ICESat footprints. Our method to estimate the total glacier areas is certainly open to discussion, but we prefer the above procedure over using areas from the Randolph Glacier Inventory because of the large deviations to our estimates, mainly for East Nyainqêntanglha and Pamir, from obviously outdated glacier outlines and voids in the Randolph inventory (Nuimura et al., 2014). The uncertainty of water equivalent quantities includes the standard error of the elevation difference trend fit, the off-glacier trends, an error due to temporal offset of the ICESat autumn campaigns from maximum cumulative ablation conditions, an uncertainty of $\pm 20\%$ for the glacier cover areas, and an uncertainty of $\pm 60 \text{ kg m}^{-3}$ for density (Kääb et al. 2012; Huss, 2013). The effects of these individual sources of uncertainty, all converted to error in mass change, are combined through the root sum of squares to arrive at the total uncertainty. Note that water equivalent results from this study are not identical to Kääb et al. (2012), even if elevation difference trends agree, due to the simplified density assumption and the different glacier area estimates used.

3.1 Comparison to gravimetric mass loss

For the Pamir, Kunlun Shan and Karakoram (zone 8b of Jacob et al., 2012; note that the Karakoram is part of their zone 8b, not 8c as suggested by their zone names) we estimate a glacier mass change of $-6 \pm 2 \text{ Gt yr}^{-1}$ for 2003-2008 that agrees well within the error with Jacob et al. (2012) results from satellite gravimetry of $-5 \pm 10 \text{ Gt yr}^{-1}$ (Jan 03-Dec 07) and $-8 \pm 9 \text{ Gt yr}^{-1}$ (Jan 04-Dec 08). For the Himalayas and East Nyainqêntanglha Shan (zone 8c of Jacob et al. 2012) we estimate a 2003-2008 glacier mass change of $-19 \pm 3 \text{ Gt yr}^{-1}$ that compares to $-3 \pm 12 \text{ Gt yr}^{-1}$ (Jan 03-Dec 07) and $-2 \pm 10 \text{ Gt yr}^{-1}$ (Jan 04-Dec 08) from satellite gravimetry. Given their fundamentally different approaches, it is challenging to discuss potential sources of disagreement between the two studies in the Himalayas and East Nyainqêntanglha. Groundwater depletion (Rodell et al., 2009), glacier imbalance runoff into endorheic basins (Zhang et al., 2013), and errors and biases in the ICESat-derived trends as discussed above and in Kääb et al. (2012) are all likely explanations. Note that Gardner et al. (2013) offer a second, more negative gravimetric estimate for the entire combined High Mountain Asia that

214 is, though, not spatially resolved enough to compare to our results. The uncertainties of our
215 results in this entire paragraph are given at 2σ confidence level to better agree with the
216 uncertainty level in Jacob et al. (2012), whereas elsewhere in this contribution uncertainty is
217 provided at 1σ confidence level.

218 **3.2 River runoff**

219 The glaciers of the Tarim Basin (only 40% of its total glacier area is covered here, with
220 notably Tien Shan missing) and the Amu Darya basin (all glacier areas covered) drain into
221 endorheic basins and thus their mass changes do not contribute to sea-level changes (Tab. 2).
222 The glacier mass changes in the Indus, Ganges and Brahmaputra basins from the present
223 study contributed together $\sim 0.06 \pm 0.01 \text{ mm yr}^{-1}$ to eustatic sea-level rise, that is $\sim 10\%$ of the
224 current sea level contribution of $0.71 \pm 0.08 \text{ mm yr}^{-1}$ from glaciers outside the ice sheets
225 (Gardner et al., 2013).

226 The discharge equivalent of these mass changes, that is the annual average glacier imbalance
227 contribution to river runoff, is given in Tab. 2 for the major river basins covered. Note that
228 computation of our discharge equivalents is a pure unit conversion from Gt yr^{-1} to $\text{m}^3 \text{ s}^{-1}$,
229 neglecting any hydrological processes and with the sole aim to roughly evaluate the relative
230 importance of glacier mass changes for river flow in the catchments.

231 The Tarim Basin glaciers most likely stored water over 2003-2008 ($+24 \pm 33 \text{ m}^3 \text{ s}^{-1}$ discharge
232 equivalent, DE). The glacier imbalance contribution to runoff is largest for Brahmaputra (-400
233 $\pm 60 \text{ m}^3 \text{ s}^{-1}$ DE), followed by the Indus ($-220 \text{ m}^3 \text{ s}^{-1}$ DE), and Ganges and Amu Darya (each -
234 $130 \text{ m}^3 \text{ s}^{-1}$ DE). Comparison of the discharge equivalent of glacier imbalance to measured
235 river runoff is increasingly biased the further downstream the gauging stations are situated
236 from the glaciers due to cumulative natural and man-made losses. It is also important to note
237 that the available runoff data from literature and databases refer to various time periods, in
238 parts considerably older than the ICESat period. Figure 2 illustrates thus only roughly the
239 hydrological significance of the 2003-2008 glacier mass change in selected gauged
240 catchments. (For details on the gauging stations used and the uncertainty of the contributions
241 see Supplement). As an example, the 2003-2008 glacier imbalance within the Upper Indus
242 basin at Besham Qila contributes $\sim 6\%$ to annual average river discharge (Fig. 2; Supplement),
243 and we roughly estimate a very similar number for the Amu Darya (Supplement). For the
244 Upper Indus basin, the hydrological balance is under ongoing discussion (cf. Reggiani and
245 Rientjes, 2014) and we hope that our glacier mass change estimates can contribute towards

246 balance closure and better understanding of spatial-temporal patterns of run-off or high-
247 elevation precipitation amounts in the region (e.g. Immerzeel et al., 2012).

248 The modelling results for “non-renewable glacier runoff” of Savoskul and Smakhtin (2013)
249 agree well with ours for Amu Darya, less for Indus (they obtain $-0.55 \text{ m w.e. yr}^{-1}$ specific
250 mass loss rate over 2001-2010, we $-0.28 \text{ m w.e. yr}^{-1}$) and Ganges (they obtain $-0.77 \text{ m w.e. yr}^{-1}$
251 ¹, we $-0.37 \text{ m w.e. yr}^{-1}$), and not very well for Brahmaputra (they obtain $-0.36 \text{ m w.e. yr}^{-1}$, we
252 $-0.90 \text{ m w.e. yr}^{-1}$).

253 4 Conclusions

254 From 2003-2008 ICESat-derived elevation difference trends over Pamir-Karakoram-
255 Himalaya and from comparison to geographically overlapping studies we draw the following
256 conclusions:

- 257 • Glacier thickness loss over the study region is most pronounced for the East
258 Nyainqêntanglha Shan, followed by the western end of the Great Himalaya Range.
259 Glaciers in and around the West Kunlun Shan are in balance or even gaining volume, and
260 Pamir and Karakoram seem to be on the western limit of this mass balance anomaly
261 rather than its centre. This suggests it is a meteorological or climatic anomaly (rise in
262 precipitation). But the cause and duration of this regional glacier anomaly is not fully
263 understood yet.
- 264 • Our glacier volume changes seem especially uncertain in Pamir and, to a lesser extent
265 Hindu Kush. The heterogeneous behaviour of individual glaciers in these two zones, for
266 instance from glacier surges, may lead to biases when extrapolating elevation difference
267 trends from particularly sparse ICESat tracks, or areas covered by differential DEMs, to
268 the entire zones.
- 269 • Extrapolation of ICESat trends back in time to the SRTM acquisition date suggests a
270 much larger potential magnitude and variability of SRTM C-band phase-centre
271 penetration than often assumed. Given the crucial importance of radar penetration for
272 glacier thickness change studies based on radar DEMs, such as the SRTM or the
273 upcoming TanDEM-X, we recommend to be critical against penetration assumptions
274 used in previous studies and to investigate the issue more extensively and systematically
275 (Langley et al., 2007; chapter 7 in Müller, 2011). The problem is complicated by the fact
276 that radar penetration has to be known specifically for certain dates from the past.

- 277 • The glacier mass changes in the Tarim and Amu Darya Basins of $+0.7 \pm 1.0 \text{ Gt yr}^{-1}$ and -
278 $4.0 \pm 0.8 \text{ Gt yr}^{-1}$ do not contribute to sea level rise. The combined Ganges, Indus and
279 Brahmaputra basin glacier mass change is $-23.7 \pm 2.1 \text{ Gt yr}^{-1}$, almost 10% of the glacier
280 contribution to sea-level rise.
- 281 • Neglecting water losses downstream of the glaciers, the 2003-2008 glacier imbalances
282 amount to ~6% of the annual discharge of Amu Darya and Upper Indus where they leave
283 the mountains. This is a considerable amount given the significance of the rivers for the
284 Aral Sea (Amu Darya), and massive irrigation schemes and household use in these dry
285 climate regions. Maximum glacier imbalance contributions to annual average river runoff
286 of up to ~17% are found for the Shyok (Indus) and ~10% Vaksh (Amu Darya), minimum
287 contributions are only ~1-3% for the monsoon-type catchments in Nepal.
- 288 • Our results on glacier mass loss agree with those from satellite gravimetry (Jacob et al.
289 2012) over Pamir, West Kunlun Shan and Karakoram, but significantly diverge over the
290 Himalaya and East Nyainqêntanglha Shan.

291 It is important to note that our results only cover 5 yr, 2003-2008, and it remains open to what
292 extent those years are representative for longer periods, such as the 10 yr covered by Gardelle
293 et al. (2013). For short mass balance series, single anomalous years may have large impacts
294 on trends. Our water equivalent results are also sensitive to density and glacier area
295 assumptions. We find that glacier outlines and areas in the study region are still quite
296 uncertain and invite the reader to use improved glacier area estimates for upscaling our
297 results, and their own assumptions for the conversion of volume changes to mass changes.

298 **Acknowledgement**

299 Sincere thanks are due to Duncan Quincey, another anonymous referee, colleagues that
300 commented on the study, and the editor Andreas Vieli for their valuable feedback that
301 certainly improved our work. The study was funded by the European Research Council under
302 the European Union's Seventh Framework Programme (FP/2007-2013) / ERC grant
303 agreement no. 320816, the ESA project Glaciers_cci (4000109873/14/I-NB), and the
304 Department of Geosciences, University of Oslo. E. Berthier acknowledges support from
305 TOSCA (CNES). We are very grateful to NASA and NSIDC for free provision for the ICESat
306 data, and the USGS for the SRTM DEM and Landsat imagery.

307

Author contributions

308

A.K. designed the study, performed the data analysis and wrote the paper. D.T., C.N and E.B.

309

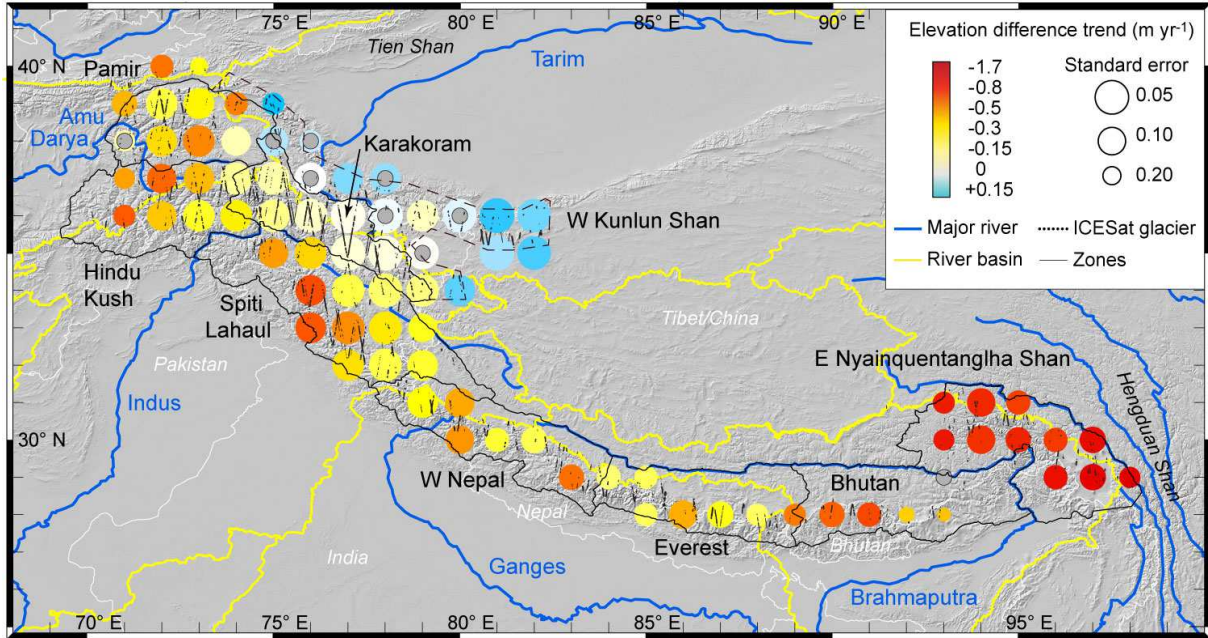
contributed to data analysis, performed supporting analyses and edited the paper.

310

311

312

Figures and Tables



313

314

315

316

317

318

319

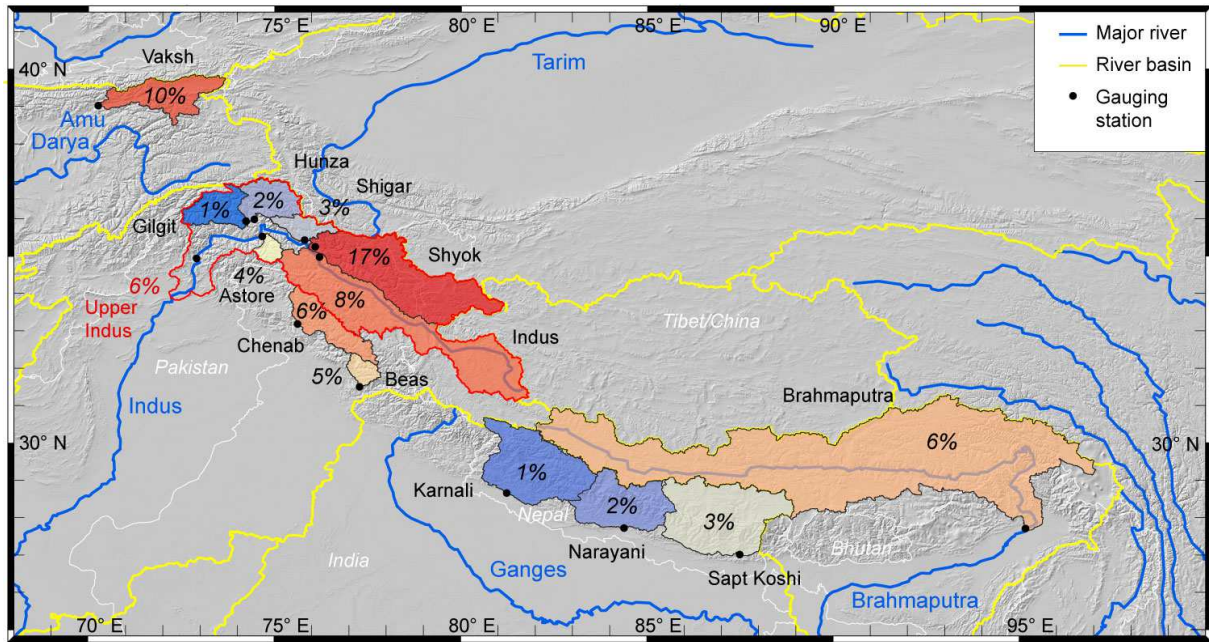
320

321

322

323

Fig. 1 Study region and trends of elevation differences during 2003–08. Data are shown on a 1° grid with overlapping rectangular geographic averaging cells of 2° × 2°. Trends are based on autumn ICESat acquisitions. Only ICESat footprints over glaciers are indicated. The zones indicated by black outlines are equivalent to the ones of Gardelle et al. (2013) with the W Kunlun Shan-Tarim zone (dashed outline) being the only additional one. Trends for all cells (coloured data circles) are statistically significant except for the cells that are marked with grey centres. The uncertainty of the temporal trends per cell is indicated through circle sizes indirectly proportional to the standard error of trends at 68% level.



325

326

327

328

329

330

331

332

Fig. 2 The percentage of discharge equivalent from annual glacier imbalance to measured average river runoff for selected catchments. Note that the actual numbers will be somewhat lower due to unaccounted water losses such as from evaporation or to groundwater. For details on the gauging stations used and the uncertainty of the contributions see Supplement.

333

334

335

336

337

338

339

340

341

Table 1: Glacier elevation difference trends over the Pamir-Karakoram-Himalaya from this and other studies. Note that Gardelle et al. (2013) cover the period 2000 to ~2010, while the other studies cover 2003 to 2008/9. Note also that the zones of this study and Gardelle et al. (2013) coincide, whereas the zones of the other do so only roughly, which can potentially explain parts of the disagreements. See text in sections 3 and 4 for an explanation of how the glacier areas were estimated. * named Hengduan Shan in Gardelle et al.(2013); ** two zones of Gardner et al. (2013) overlap with our zone and both their values are given.

Zone	Glacier area (km ²)	This study (m yr ⁻¹ , ± at 1σ-level)	Gardner et al. (2013; m yr ⁻¹ , ± at 2σ-level)	Neckel et al. (2014; m yr ⁻¹ , ± at 1σ-level)	Gardelle et al. (2013; m yr ⁻¹ , ± at 1σ-level)
East Nyainqêntanglha *	6000	-1.34 ±0.29	-0.30 ±0.13 -0.40 ±0.41 **	-0.81±0.32	-0.39 ± 0.16
Bhutan	3500	-0.89 ±0.16	-0.89 ±0.18	-0.78 ±0.27	-0.26 ± 0.15
Everest	8500	-0.37 ±0.10	-0.44 ±0.20		-0.30 ± 0.16
West Nepal	7500	-0.43 ±0.09		-0.44 ±0.26	-0.38 ± 0.16
Spiti Lahaul	9500	-0.49 ±0.12	-0.53 ±0.13		-0.53 ± 0.16
Karakoram	21000	-0.10 ±0.06	-0.12 ±0.15		+0.12 ± 0.19
Hindu Kush	5500	-0.49 ±0.10			-0.14 ± 0.19
Pamir	6500	-0.48 ±0.14	-0.13 ±0.22		+0.16 ± 0.15
West Kunlun Shan - Tarim	12500	+0.05 ±0.07	+0.17 ±0.15	+0.04 ±0.29	
Area-weighted mean	80500	-0.37 ±0.10			

342

343

344

345

346

347

348

349

Table 2: Glacier thickness and mass changes over the major river basins of the study area. The discharge equivalent is a unit conversion from mass change and neglects any losses such as by evaporation or to groundwater. (i) The Tarim Basin is endorheic. Only parts of the glacier area (~40%) within the Tarim Basin are covered in this study. (ii) Endorheic basin.

Major river basin	Glacier area (km ²)	Elevation difference trend (m yr ⁻¹)	Mass change (Gt yr ⁻¹)	Discharge equivalent DE (m ³ s ⁻¹)
Tarim ⁽ⁱ⁾	15000	+0.06 ± 0.08	+0.7 ± 1.0	+24 ± 33
Amu Darya ⁽ⁱⁱ⁾	11000	-0.43 ± 0.08	-4.0 ± 0.8	-128 ± 25
Indus	25000	-0.33 ± 0.04	-7.0 ± 0.8	-220 ± 26
Ganges	11000	-0.44 ± 0.07	-4.1 ± 0.6	-130 ± 20
Brahmaputra	14000	-1.06 ± 0.15	-12.6 ± 1.9	-400 ± 60

350

351

References

- Becker, A., Finger, P., Meyer-Christoffer, A., Rudolf, B., Schamm, K., Schneider, U., and Ziese, M.: A description of the global land-surface precipitation data products of the Global Precipitation Climatology Centre with sample applications including centennial (trend) analysis from 1901–present, *Earth Syst. Sci. Data*, 5, 71–99, 10.5194/essd-5-71-2013, 2013.
- Bolch, T., Kulkarni, A., Kääb, A., Huggel, C., Paul, F., Cogley, J.G., Frey, H., Kargel, J.S., Fujita, K., Scheel, M., Bajracharya, S. and Stoffel, M. The state and fate of Himalayan glaciers. *Science*. 336, 310–314, 2012.
- Cogley, J. G.: Present and future states of Himalaya and Karakoram glaciers, *Ann. Glaciol.*, 52, 69–73, 2011.
- Dall, J., Madsen, S. N., Keller, K. and Forsberg, R.: Topography and penetration of the Greenland Ice Sheet measured with airborne SAR interferometry, *Geophysical Research Letters*, 28(9), 1703–1706, 2001.
- Fujita, K.: Effect of precipitation seasonality on climatic sensitivity of glacier mass balance, *Earth Planet. Sc. Lett.*, 276, 14–19, 10.1016/j.epsl.2008.08.028, 2008.
- Gardelle, J., Berthier, E. and Arnaud, Y. Slight mass gain of Karakoram glaciers in the early 21st century. *Nature Geoscience*. 5, 322–325, 2012.
- Gardelle, J., Berthier, E. and Arnaud, Y.: Impact of resolution and radar penetration on glacier elevation changes computed from multi-temporal DEMs, *Journal of Glaciology*, 58(208), 419–422, 2012.
- Gardelle, J., Berthier, E., Arnaud, Y. and Kääb, A. Region-wide glacier mass balances over the Pamir-Karakoram-Himalaya during 1999–2011. *The Cryosphere*. 7, 1263–1286, 2013
- Gardner, A.S., Moholdt, G., Cogley, J.G., Wouters, B., Arendt, A.A., Wahr, J., Berthier, E., Hock, R., Pfeffer, W.T., Kaser, G., Ligtenberg, S.R.M., Bolch, T., Sharp, M.J., Hagen, J.O., van den Broeke, M.R. and Paul, F. A reconciled estimate of glacier contributions to sea level rise: 2003 to 2009. *Science*. 340(6134), 852–857, 2013.
- Hewitt, K. Glacier change, concentration, and elevation effects in the Karakoram Himalaya, Upper Indus Basin. *Mountain Research and Development*. 31(3), 188–200, 2011.
- Huss, M. Density assumptions for converting geodetic glacier volume change to mass change. *The Cryosphere*. 7(3), 877–887, 2011.
- Immerzeel, W.W., Pellicciotti, F. and Shrestha, A.B. Glaciers as a proxy to quantify the spatial distribution of precipitation in the Hunza basin. *Mountain Research and Development*. 32(1), 30–38, 2012.
- Jacob, T., Wahr, J., Pfeffer, W.T. and Swenson, S. Recent contributions of glaciers and ice caps to sea level rise. *Nature*. 482, 514–518, 2012.
- Kääb, A., Berthier, E., Nuth, C., Gardelle, J. and Arnaud, Y. Contrasting patterns of early twenty-first-century glacier mass change in the Himalayas. *Nature*. 488(7412), 495–498, 2012.
- Kapnick, S. B., Delworth, T. L., Ashfaq, M., Malyshev, S., and Milly, P. C. D.: Snowfall less sensitive to warming in Karakoram than in Himalayas due to a unique seasonal cycle, 7, 834–840, 10.1038/ngeo2269, 2014

- 397 Langley, K., Hamran, S. E., Hogda, K. A., Storvold, R., Brandt, O., Hagen, J. O., and Kohler,
398 J.: Use of C-band ground penetrating radar to determine backscatter sources within
399 glaciers, *Ieee T Geosci Remote*, 45, 1236-1246, Doi 10.1109/Tgrs.2007.892600, 2007.
- 400 Loibl, D., Lehmkuhl, F., and Griessinger, J.: Reconstructing glacier retreat since the Little Ice
401 Age in SE Tibet by glacier mapping and equilibrium line altitude calculation,
402 *Geomorphology*, 214, 22-39, DOI 10.1016/j.geomorph.2014.03.018, 2014.
- 403 Maussion, F., Scherer, D., Mölg, T., Collier, E., Curio, J., and Finkelnburg, R.: Precipitation
404 seasonality and variability over the Tibetan Plateau as resolved by the High Asia
405 Reanalysis, *J Climate*, 27, 1910-1927, Doi 10.1175/Jcli-D-13-00282.1, 2014.
- 406 Müller, K.: Microwave penetration in polar snow and ice: implications for GPR and SAR,
407 Dissertation, Faculty of Mathematics and Natural Sciences. University of Oslo,
408 available from <http://www.duo.uio.no/>, 2011.
- 409 Neckel, N., Kropacek, J., Bolch, T. and Hochschild, V. Glacier mass changes on the Tibetan
410 Plateau 2003-2009 derived from ICESat laser altimetry measurements. *Environmental*
411 *Research Letters*. 9(1), 2014
- 412 Nuimura, T., Sakai, A., Taniguchi, K., Nagai, H., Lamsal, D., Tsutaki, S., Kozawa, A.,
413 Hoshina, Y., Takenaka, S., Omiya, S., Tsunematsu, K., Tshering, P., and Fujita, K.:
414 The GAMDAM Glacier Inventory: a quality controlled inventory of Asian glaciers,
415 *The Cryosphere*, 8, 2799-2829, 10.5194/tcd-8-2799-2014, 2014.
- 416 Pelto, M. S.: Forecasting temperate alpine glacier survival from accumulation zone
417 observations, *The Cryosphere*, 4, 67-75, 2010.
- 418 Pfeffer, W. T., Arendt, A. A., Bliss, A., Bolch, T., Cogley, J. G., Gardner, A. S., Hagen, J. O.,
419 Hock, R., Kaser, G., Kienholz, C., Miles, E. S., Moholdt, G., Molg, N., Paul, F.,
420 Radic, V., Rastner, P., Raup, B. H., Rich, J., Sharp, M. J., Andeassen, L. M.,
421 Bajracharya, S., Barrand, N. E., Beedle, M. J., Berthier, E., Bhambri, R., Brown, I.,
422 Burgess, D. O., Burgess, E. W., Cawkwell, F., Chinn, T., Copland, L., Cullen, N. J.,
423 Davies, B., De Angelis, H., Fountain, A. G., Frey, H., Giffen, B. A., Glasser, N. F.,
424 Gurney, S. D., Hagg, W., Hall, D. K., Haritashya, U. K., Hartmann, G., Herreid, S.,
425 Howat, I., Jiskoot, H., Khromova, T. E., Klein, A., Kohler, J., König, M., Kriegel, D.,
426 Kutuzov, S., Lavrentiev, I., Le Bris, R., Li, X., Manley, W. F., Mayer, C., Menounos,
427 B., Mercer, A., Mool, P., Negrete, A., Nosenko, G., Nuth, C., Osmonov, A.,
428 Pettersson, R., Racoviteanu, A., Ranzi, R., Sarikaya, M. A., Schneider, C., Sigurdsson,
429 O., Sirguey, P., Stokes, C. R., Wheate, R., Wolken, G. J., Wu, L. Z., Wyatt, F. R., and
430 Consortium, R.: The Randolph Glacier Inventory: a globally complete inventory of
431 glaciers, *J Glaciol*, 60, 537-552, Doi 10.3189/2014jog13j176, 2014.
- 432 Reggiani P. and T. H. M. Rientjes (2014). A reflection on the long-term water balance of the
433 Upper Indus Basin. *Hydrology Research*. In press.
- 434 Rignot, E., Echelmeyer, K. and Krabill, W. Penetration depth of interferometric synthetic-
435 aperture radar signals in snow and ice. *Geophysical Research Letters*. 28(18), 3501-
436 3504, 2001.
- 437 Rodell, M., Velicogna, I. and Famiglietti, J.S. Satellite-based estimates of groundwater
438 depletion in India. *Nature*. 460(7258), 999-1002, 2009.
- 439 Sakai, A., Nuimura, T., Fujita, K., Takenaka, S., Nagai, H., and Lamsal, D.: Climate regime
440 of Asian glaciers revealed by GAMDAM Glacier Inventory, *The Cryosphere*, 8, 3629-
441 3663, 10.5194/tcd-8-3629-2014, 2014.
- 442 Sarikaya, M.A., Bishop, M.P., Shroder, J.F. and Olsenholler, J.A. Space-based observations
443 of Eastern Hindu Kush glaciers between 1976 and 2007, Afghanistan and Pakistan.
444 *Remote Sensing Letters*. 3(1), 77-84, 2012.
- 445 Savoskul, O. S., and Smakhtin, V.: Glacier systems and seasonal snow cover in six major
446 Asian river basins: hydrological role under changing climate, *International Water*
447 *Management Institute (IWMI), Colombo, Sri Lanka*. 150, 2013.

- 448 Yao, T.D., Thompson, L., Yang, W., Yu, W.S., Gao, Y., Guo, X.J., Yang, X.X., Duan, K.Q.,
449 Zhao, H.B., Xu, B.Q., Pu, J.C., Lu, A.X., Xiang, Y., Kattel, D.B. and Joswiak, D.
450 Different glacier status with atmospheric circulations in Tibetan Plateau and
451 surroundings. *Nature Climate Change*. 2(9), 663-667, 2012.
- 452 Yi, S. and Sun, W.: Evaluation of glacier changes in high-mountain Asia based on 10 year
453 GRACE RL05 models, *Journal of Geophysical Research: Solid Earth*, 119(3),
454 2013JB010860, 2013.
- 455 Tao, H., Borth, H., Fraedrich, K., Su, B., & Zhu, X. Drought and wetness variability in the
456 Tarim River Basin and connection to large-scale atmospheric circulation. *International*
457 *Journal of Climatology*, 34: 2678 – 2684, 2014.
- 458 Zhang, G.Q., Yao, T.D., Xie, H.J., Kang, S.C. and Lei, Y.B. Increased mass over the Tibetan
459 Plateau: From lakes or glaciers? *Geophysical Research Letters*. 40(10), 2125-2130,
460 2013.
- 461
- 462

Supplement

464 The gauging stations used for the results shown in Fig. 2 are listed in Tab. S1. Reliable river
 465 runoff data are notoriously difficult to obtain over and around the Himalayas. Even if
 466 available, their use and distribution are sometimes restricted. As example catchments we
 467 select therefore only the ones where discharge data stem from peer-reviewed studies, or where
 468 the data were used in peer-reviewed studies, and where the data cover sufficiently long time
 469 periods. It is outside the focus of the present brief communication to compile a geographically
 470 complete set of catchment discharge data. The uncertainty of the glacier imbalance
 471 contribution to river runoff (Fig. 2) is estimated in the same way as the uncertainty of glacier
 472 mass changes, but uncertainties in the river runoff data used are neglected.

473

474 **Table S1.** Gauging stations indicated in Fig. 2 and uncertainty of our percentage
 475 discharge contributions of glacier imbalance to river runoff at 1σ -level.

476

River	Gauging station	Annual discharge ($\text{m}^3 \text{s}^{-1}$)	Period of measurements	Source	Uncertainty of percentage discharge contributions
Vaksh	Garm	320	1933-1990	Global Runoff Data Centre (GRDC)	$\pm 5\%$
Gilgit	Gilgit	287	1980-2010	Mukhopadhyay and Khan (2014)	$\pm 2\%$
Hunza	Dainyor Bridge	332	1966-2010	"	$\pm 2\%$
Shigar	Shigar	203	1985-1998	"	$\pm 2\%$
Astore	Doyian	136	1974-2009	"	$\pm 2\%$
Upper Indus	Kharmong	452	1982-2010	"	$\pm 3\%$
Shyok	Yogo	362	1973-2010	"	$\pm 6\%$
Upper Indus	Besham Qila	2431	1969-2010	"	$\pm 2\%$
Chenab	Prem Nagar	626	1968-1986	Hofer (1993)	$\pm 3\%$
Beas	Thalout	190	1997-2001	Liu et al. (2013)	$\pm 2\%$
Karnali	Chisapani	1350	1962-1993	GRDC	$\pm 1\%$
Narayani	Narayangh	1590	1963-2006	Collins et al. (2013)	$\pm 1\%$
Sapt Koshi	Chatara	1537	1977-	GRDC	$\pm 1\%$
Brahmaputra	Pasighat	5870	1949-1962, 1976-1978	Sarma (2005)	$\pm 2\%$
Amu Darya	ungauged	~ 2300	"long-term mean"	http://www.cawater-info.net ; Agal'tseva et al. (2011)	$\pm 1\%$

477

- 479 Agal'tseva, N.A., Bolgov M.V., Spektorman T.Yu., Trubetskova M.D., and Chub V.E.
480 Estimating hydrological characteristics in the Amu Darya River basin under climate
481 change conditions. *Russian Meteorology and Hydrology*. 36(10), 681-689, 2011.
- 482 Collins, D. N., Davenport, J. L. and Stoffel, M.. Climatic variation and runoff from partially-
483 glacierised Himalayan tributary basins of the Ganges. *Science of the Total*
484 *Environment*, 468, 48-59, 2013.
- 485 GRDC. Global Runoff Data Centre. Composite runoff fields v1.0.
486 <http://www.grdc.sr.unh.edu/index.html>.
- 487 Hofer, T. Himalayan deforestation, changing river discharge, and increasing floods: myth or
488 reality? *Mountain Research and Development*, 213-233, 1993.
- 489 Li Lu, Engelhardt M., Xu Chong-Yu., Jain S. K. and Singh V. P. Comparison of satellite-
490 based and reanalyzed precipitation as input to glacio-hydrological modeling for Beas
491 river basin, Northern India. – Cold and Mountain Region Hydrological Systems Under
492 Climate Change: Towards Improved Projections, Proceedings of H02, IAHS-IAPSO-
493 IASPEI Assembly, July 2013, Gothenburg, Sweden), International Association of
494 Hydrological Sciences (IAHS) Publication number 360, 45-52, 2013.
- 495 Mukhopadhyay, B., and Khan, A.: A quantitative assessment of the genetic sources of the
496 hydrologic flow regimes in Upper Indus Basin and its significance in a changing
497 climate, *J Hydrol*, 509, 549-572, DOI 10.1016/j.jhydrol.2013.11.059, 2014.
- 498 Sarma, J. N. Fluvial process and morphology of the Brahmaputra River in Assam, India.
499 *Geomorphology*, 70(3), 226-256, DOI: 10.1016/j.geomorph.2005.02.007, 2005.